

Article

Effect of Thermal Distress on Residual Behavior of CFRP-Strengthened Steel Beams Including Periodic Unbonded Zones

Isamu Yoshitake ^{1,*}, Hisatsugu Tsuda ^{2,†}, Yail J. Kim ^{3,†} and Nobuhiro Hisabe ^{4,†}

Received: 29 June 2015 ; Accepted: 12 November 2015 ; Published: 17 November 2015

Academic Editor: Raafat El-Hacha

¹ Department of Civil and Environmental Engineering, Yamaguchi University, 2-16-1 Tokiwadai, Ube, Yamaguchi 755-8611, Japan

² IHI Infrastructure Systems Co., Ltd., 3 Ohama Nishimachi, Sakai, Osaka 590-0977, Japan; hisatsugu_tsuda@iis.ihi.co.jp

³ Department of Civil Engineering, University of Colorado Denver, Denver, CO 80217, USA; jimmy.kim@ucdenver.edu

⁴ Mitsubishi Plastics Infratec Co., Ltd., 1-2-2 Nihonbashihongokuchō, Chuo-ku, Tokyo 103-0021, Japan; hisabe.nobuhiro@mb.mpi.co.jp

* Correspondence: yositake@yamaguchi-u.ac.jp; Tel.: +81-836-85-9306; Fax: +81-836-85-9301

† These authors contributed equally to this work.

Abstract: This paper presents the residual behavior of wide-flange steel beams strengthened with high-modulus carbon fiber-reinforced polymer (CFRP) laminates subjected to thermal loading. Because the coefficients of thermal expansion of the steel and the CFRP are different, temperature-induced distress may take place along their interface. Periodic unbonded zones are considered to represent local interfacial damage. Five test categories are designed depending on the size of the unbonded zones from 10 to 50 mm, and corresponding beams are loaded until failure occurs after exposing to a cyclic temperature range of $\Delta T = 25$ °C (−10 to 15 °C) up to 84 days. The composite action between the CFRP and the steel substrate is preserved until yielding of the beams happens, regardless of the thermal cycling and periodic unbonded zones. The initiation and progression of CFRP debonding become apparent as the beams are further loaded, particularly at geometric discontinuities in the vicinity of the unbonded zones along the interface. A simple analytical model is employed to predict the interfacial stress of the strengthened beams. A threshold temperature difference of $\Delta T = 30$ °C is estimated for the initiation and progression of CFRP debonding. Multiple debonding-progression stages in conjunction with the extent of thermal distress appear to exist. It is recommended that high-modulus CFRP be restrictively used for strengthening steel members potentially exposed to a wide temperature variation range.

Keywords: carbon fiber-reinforced polymer; interfacial stress; steel; strengthening; thermal coefficient

1. Introduction

High-modulus carbon fiber-reinforced polymer (CFRP) laminates may be used for strengthening constructed steel girder bridges. Polymeric adhesives are typically employed to bond the laminates to a steel substrate in order to enhance flexural capacity. Numerous structural advantages are associated with such a strengthening method, including easy and rapid installation, minimal disturbance to traffic, fatigue resistance and tailorability for irregular geometry [1]. The interface between the CFRP and steel substrate is often degraded during the service life of strengthened members, because a variety of environmental factors (e.g., temperature, moisture, and ultraviolet rays) cause chemical

or mechanical distress. Previous research asserts that the mechanical and rheological characteristics of CFRP and bonding agents altered when aggressive environments were imposed [2,3]. Interfacial responses are also influenced by service conditions as reported by the following selected literature. Dawood and Rizkalla [4] tested double-lap joints in corrosive environments. Various bonding schemes were utilized in addition to conventional CFRP-steel bonding with an epoxy adhesive: silane and glass FRP (GFRP) layers were positioned in between the steel and the CFRP. Upon completing four months of exposure to wet-dry and 5% NaCl at 38 °C, the joints were tensioned until failure happened. The primary contribution to decreasing the strength of the joints was the degraded CFRP-steel interface, while deterioration of the bonding agent was a secondary attribute. The specimens having silane layers exhibited better performance compared to those with GFRP layers. Al-Shawaf [5] developed a finite element model using a commercial software to predict the behavior of the CFRP-steel interface in elevated temperatures ranging from –40 to 60 °C. A heat transfer mechanism was taken into account in conjunction with the experimentally-measured thermal properties of the constituent materials. Failure criteria were established to represent the fracture or yielding of the interface model. Strains along the bond-line and interfacial strength were estimated. Although some margin was noticed between the predicted and tested results, the proposed approach was generally acceptable. Nguyen *et al.* [6] examined the time-dependent response of a CFRP-steel interface exposed to thermal and mechanical loading. Multiple testing scenarios were planned, namely a constant temperature of 35 °C, variable temperatures from 40 to 50 °C, and cyclic thermal loading between 20 and 50 °C, combined with constant mechanical tension. Dynamic mechanical analysis (DMA) was carried out to measure the thermal properties of adhesive materials. Empirical equations were developed to evaluate the degradation of the adhesives. The time to failure was substantially affected by the extent of the applied mechanical load and the degree of thermal exposure. Mechanics-based theoretical investigations into the interfacial bond between the CFRP and concrete substrate were studied by several researchers. Rabinovitch [7] developed an analytical model for CFRP-strengthened concrete beams at elevated temperatures from –10 to 80 °C, based on high-order mathematical equations combined with a fracture mechanics approach. Predicted results included stress profiles along the bond-line, failure load, and edge debonding. With an increase in temperature, the strength of the CFRP-concrete interface was reduced. Gao *et al.* [8] studied the effect of temperature variation on the behavior of CFRP-concrete interface using a pull-out element configuration, from –10 to 50 °C. A bi-linear bond slip-model was discussed to examine the debonding issue of the interface. Thermal loading influenced the development of a debonding zone. Gao *et al.* [9] expanded the modeling approach with various bond-slip relationships, such as elastic-brittle, trapezoidal, rigid-softening, elastic-perfectly plastic, and exponential cases. These bond-slip models were found to be insensitive to thermal loading, whereas they affected the size of effective bond length.

As stated above, the primary focus of existing research with regard to CFRP-strengthened steel members in environmental loading is on examining the behavior of CFRP-steel interface at an element level (*i.e.*, coupon testing) and on theoretically evaluating the response of concrete beams strengthened with CFRP. Investigations at a structure level are reported rarely, particularly scarce for steel structures, and further research is necessary accordingly. This paper discusses a test program concerning the performance of CFRP-strengthened steel beams subjected to temperature-induced distress with an emphasis on their residual behavior. Periodic bond deterioration was intentionally created to experimentally simulate the occurrence of local CFRP debonding, and the corresponding consequences were studied.

2. Research Significance

Strain discrepancy between the CFRP and steel caused by their different coefficients of thermal expansion appears to be a detrimental factor when a strengthened beam is exposed to variable temperatures. This issue may become more apparent for high-modulus CFRP materials, provided

that their coefficient of thermal expansion is significantly lower than that of structural steel. The performance of the CFRP-steel interface and the flexural behavior of the strengthened beam in such an exposure condition should be examined to clarify the effect of temperature-induced distress. Synergetic deterioration with partial CFRP debonding that could happen along the interface is another important technical aspect to understand the long-term durability of the CFRP system.

3. Methodology

3.1. Test Specimens

Typical mild steel wide-flange beams (“H-beam”) were used for experimental investigations. High-modulus CFRP laminates were bonded to the tensile soffit of the beam using a structural epoxy, as shown in Figure 1a. The dimensions of the H-beam and the CFRP laminate were 100 mm wide, 100 mm high, 1600 mm long and 100 mm wide, 2 mm thick, and 1600 mm long, respectively.

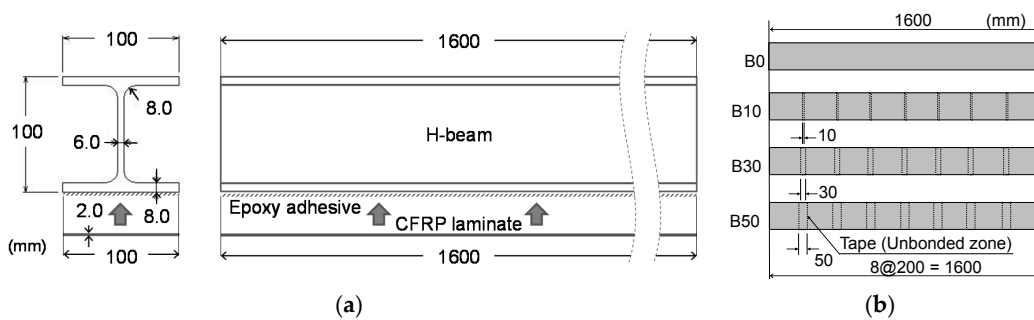


Figure 1. Beam details: (a) side view; (b) bottom view.

Tables 1 and 2 reveal the engineering properties of the respective materials. The surface of each beam was prepared using an electric grinder, and the CFRP laminate was bonded (Figure 2a). The epoxy thickness measured was 0.2 mm, on average. To examine the effect of premature local CFRP debonding, periodic unbonded zones were created along the bond-line of the CFRP (Figure 1b) having a width of 10, 30 and 50 mm. General-purpose duct tape was used to avoid bonding between the steel substrate and the CFRP, as shown in Figure 2b. All strengthened beams were cured for 10 days at room temperature according to the recommendation of the adhesive manufacturer. The beam specimens were categorized into five groups depending on the strengthening schemes and the width of the unbonded zone (Table 3), including one control and four strengthened beams. Beam B0 had complete CFRP bonding along the lower flange, while Beams B10, B30, and B50 had partial discontinuities due to use of the duct tape. One beam specimen was used for each test, and 13 beams were tested in total.

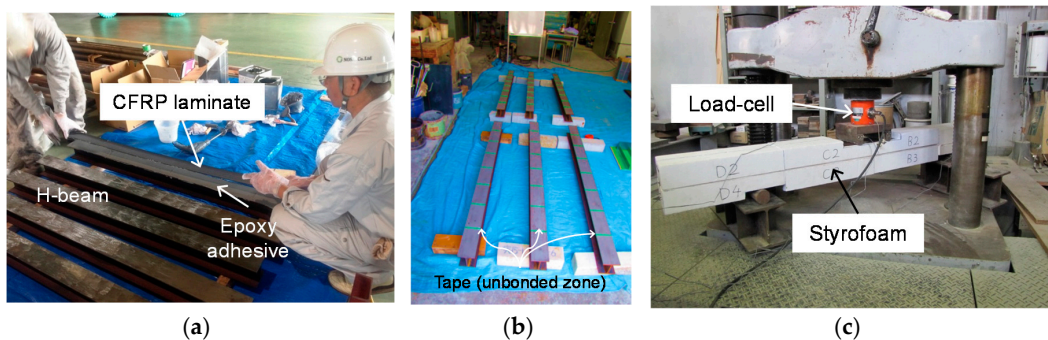


Figure 2. Specimen preparation and test setup: (a) CFRP bonding; (b) creation of the periodic unbonded zone along the beam; (c) flexural test.

Table 1. Nominal material properties for steel beam and CFRP.

Properties	H-Beam	CFRP laminate
Yield strength or tensile strength	245 MPa	1628 MPa
Young’s modulus	200 GPa	480 GPa
Poisson’s ratio	0.3	0.3
Coefficient of thermal expansion (CTE)	$12.0 \times 10^{-6}/^{\circ}\text{C}$	$0.3 \times 10^{-6}/^{\circ}\text{C}$

Table 2. Properties of epoxy adhesive.

Properties	Value
Density	1.7 g/cm ³
Unit weight	375 g/m ²
Useable bonding time	84 min
Shear strength	16.0 MPa
Bond strength	3.7 MPa
Compressive strength	65 MPa
Young’s modulus	4.9 GPa
Poisson’s ratio	0.4
Coefficient of thermal expansion	$68 \times 10^{-6}/^{\circ}\text{C}$

Table 3. Beam specimens and test parameters.

Identification	Number of Beams Tested	Unbonded Zone	Flexural Test Time
Control	1	N/A	at 0 day
B0	3	None	at 0, 28, 84 days
B10	3	7@100 × 10 mm	at 0, 28, 84 days
B30	3	7@100 × 30 mm	at 0, 28, 84 days
B50	3	7@100 × 50 mm	at 0, 28, 84 days

3.2. Temperature Cycling

An environmental chamber with a digital temperature adjustment feature was employed to cycle variable temperatures from -10 to 15 °C ($\Delta T = 25$ °C), as shown in Figure 3a. Thermocouples were bonded to the beam to monitor the variation of the temperature (Figure 3b). The initial temperature of -10 °C was maintained for Beam B0 for 7 days (Figure 4a), after which other beams were placed inside the chamber (Figure 4b), and a typical temperature cycle for 7 days was proceeded up to 12 weeks or 84 days. It is worth noting that there is no specific standard test protocol for such experimental investigations, while the temperature range and exposure period were determined according to previous research [10].

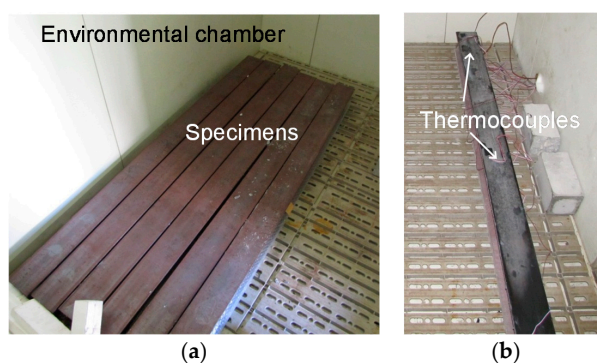


Figure 3. Thermal cycling in an environmental chamber: (a) test in progress; (b) thermocouples to monitor temperature variation.

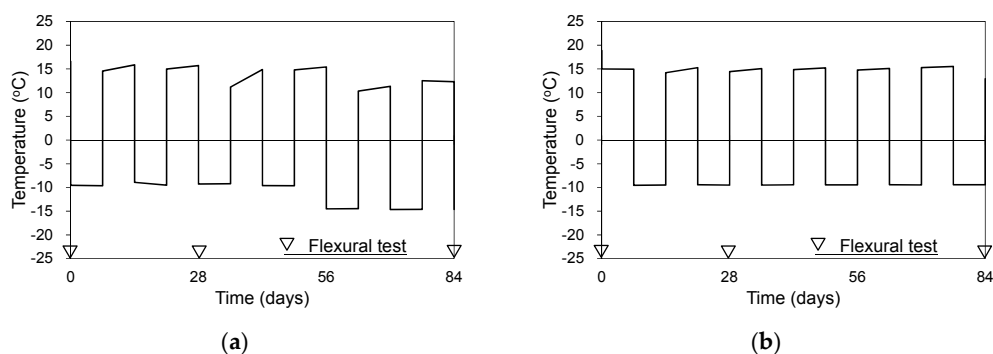


Figure 4. Temperature variation: (a) Beam B0; (b) Beams B10, B30 and B50.

3.3. Flexural Test

Upon achieving certain thermal cycles (*i.e.*, 0, 28 and 84 days), the conditioned beams were mechanically loaded in four-point bending. A load rate of 0.2 kN/s was adopted. The beams were covered with Styrofoam to minimize the effect of ambient temperature (Figure 2c), so that the state of the CFRP-steel interface could be preserved even though the testing was conducted outside the environmental chamber. Strain gages were bonded to the steel and CFRP as depicted in Figure 5. Provided that the technical interest of the present experimental program was in thermal effects combined with partial CFRP debonding along the CFRP-steel interface, rather than in conventional end-peeling failure, the supports were positioned at a distance of 270 mm away from beam-end to preclude premature end-peeling.

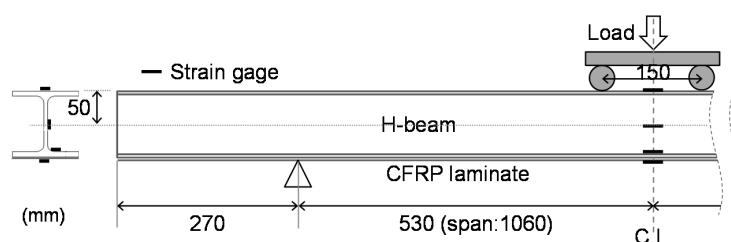


Figure 5. Schematic of the flexural test and instrumentation. C.L., Center Line.

4. Results and Discussion

4.1. Residual Capacity

Figure 6 displays the residual capacity of the strengthened beams loaded at 0, 28 and 84 days of exposure to thermal distress. The yield load of the strengthened beams without experiencing thermal cycles (zero days) was 31% higher than that of the control beam, on average, as shown in Figure 6a. Such a trend was generally maintained irrespective of exposure time; for instance, the B50 category tested at 28 and 84 days revealed 30% and 29% higher yield loads compared with the control counterpart. This fact corroborates that the applied tensile stress in the vicinity of the lower flange was shared by the steel and the CFRP until the strengthened beams yielded; in other words, the composite action along the CFRP-steel interface was not significantly influenced by the thermal cycling prior to yielding of the beams, even though partial CFRP debonding (unbonded zone) was periodically present. The progression of CFRP debonding from the unbonded zones was not observed until yielding took place. Unlike the yield-load case discussed above, the ultimate capacity of the strengthened beams fluctuated to a relatively large extent (Figure 6b). This is attributed to the fact that the local flange yielding of the beams was associated with the progression of CFRP debonding. Local damage occurring at the geometric discontinuities where the unbonded zone existed was activated

and propagated as the load stage of the beam migrated from yielding to ultimate. A preliminary conclusion made from these observations is that local CFRP debonding along the CFRP-steel interface may not be a critical factor in service; however, the debonding can propagate along the interface as temperature-induced damage accumulates and, thus, can affect the capacity of the strengthened beam. Additional experimental confirmation is necessary to generalize this assertion, because the number of test specimens was limited in this research program.

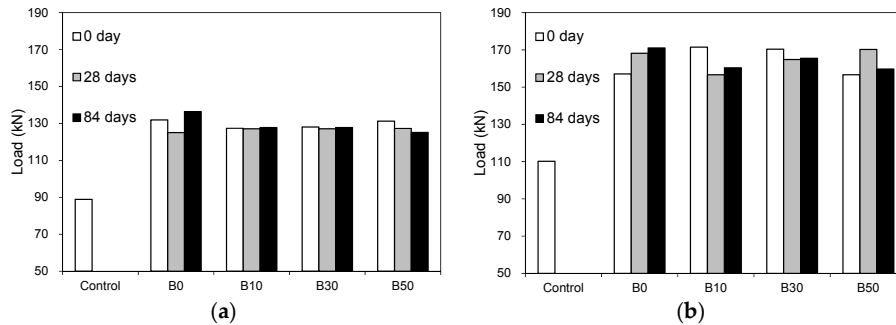


Figure 6. Residual load-carrying capacity of test beams: (a) yield load; (b) ultimate load.

4.2. Load-Strain Behavior

Figures 7–9 demonstrate the load-strain behavior of the test beams. The compression and tension strains measured at the upper and lower flanges of the strengthened beams were essentially identical to those of the control within their comparable range. This indicates that the strain compatibility of the strengthened beams was maintained regardless of thermal cycling and further confirms the aforementioned full-composite action up to yielding of the beams. It may be of interest to state that the range of strain development in the strengthened beam with 50-mm unbonded zones (Figure 9d) was narrower than that of other beams. Such a fact points out that stress transfer from the steel to the CFRP was not effective as the level of local damage increased, because the internal energy of Beam B50 was partially dissipated along the CFRP-steel interface via the unbonded zones.

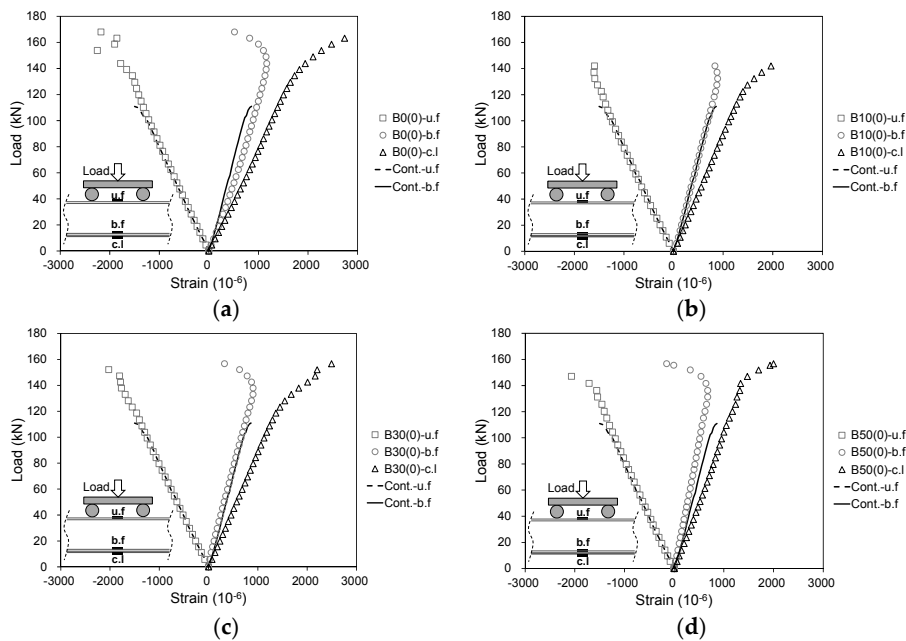


Figure 7. Load-strain responses of beams tested at zero days: (a) Beam B0; (b) Beam B10; (c) Beam B30; (d) Beam B50.

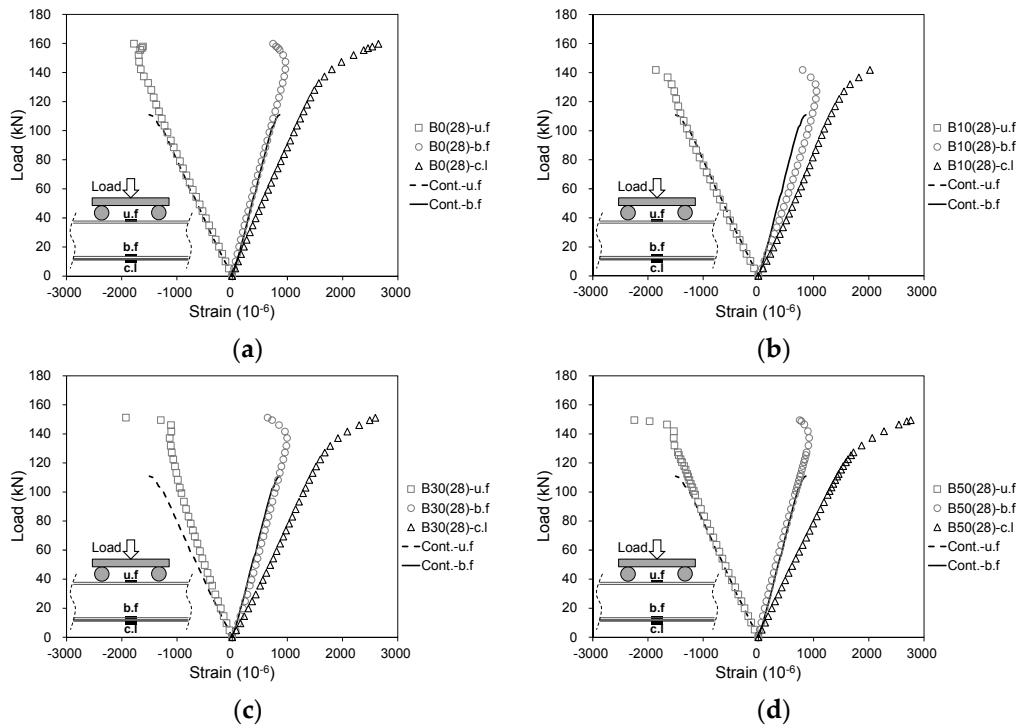


Figure 8. Load-strain responses of beams tested at 28 days: (a) Beam B0; (b) Beam B10; (c) Beam B30; (d) Beam B50.

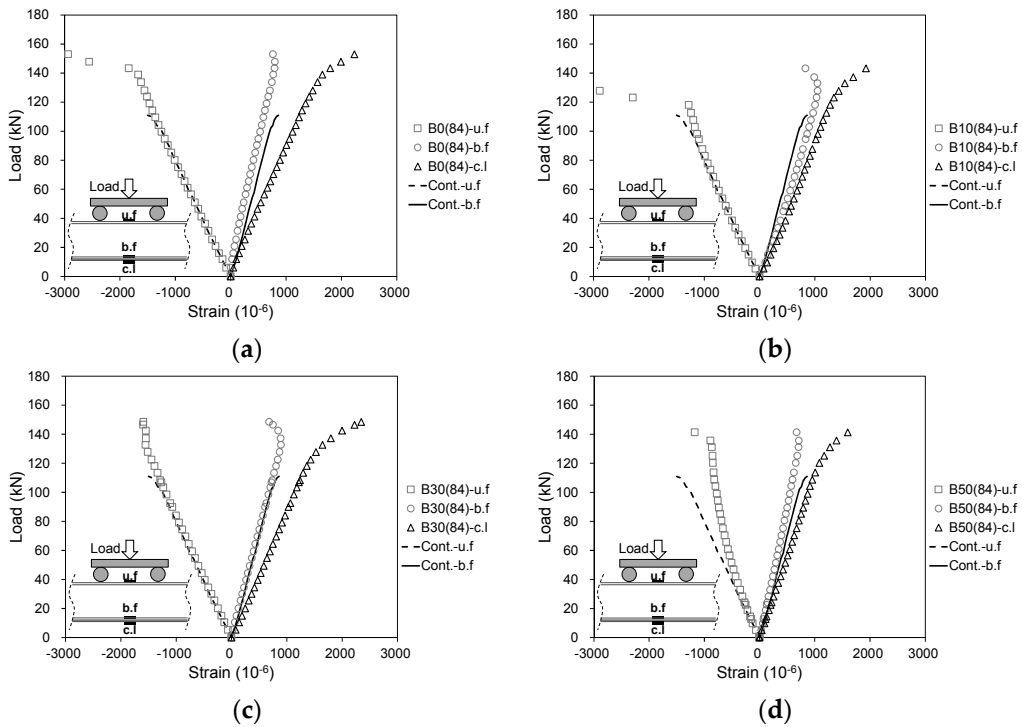


Figure 9. Load-strain responses of beams tested at 84 days: (a) Beam B0; (b) Beam B10; (c) Beam B30; (d) Beam B50.

4.3. Failure Mode

A pictorial summary for the failure mode of the strengthened beams is given in Figure 10. In all cases, explicit CFRP rupture was noticed (Figure 10a) because the laminate was intentionally restrained by the supports (Figure 5). It is again noted that the focus of the experimental study was on the effect of local debonding along the CFRP-steel interface subjected to thermal distress, rather than examining typical end-peeling failure of the CFRP. Figure 10b exhibits the initiation and progression of CFRP debonding within the constant moment region due to the presence of the unbonded zone, entailing stress concentrations. All tested beams revealed significant irreversible damage evidenced by the permanent deformation available in Figure 10c.

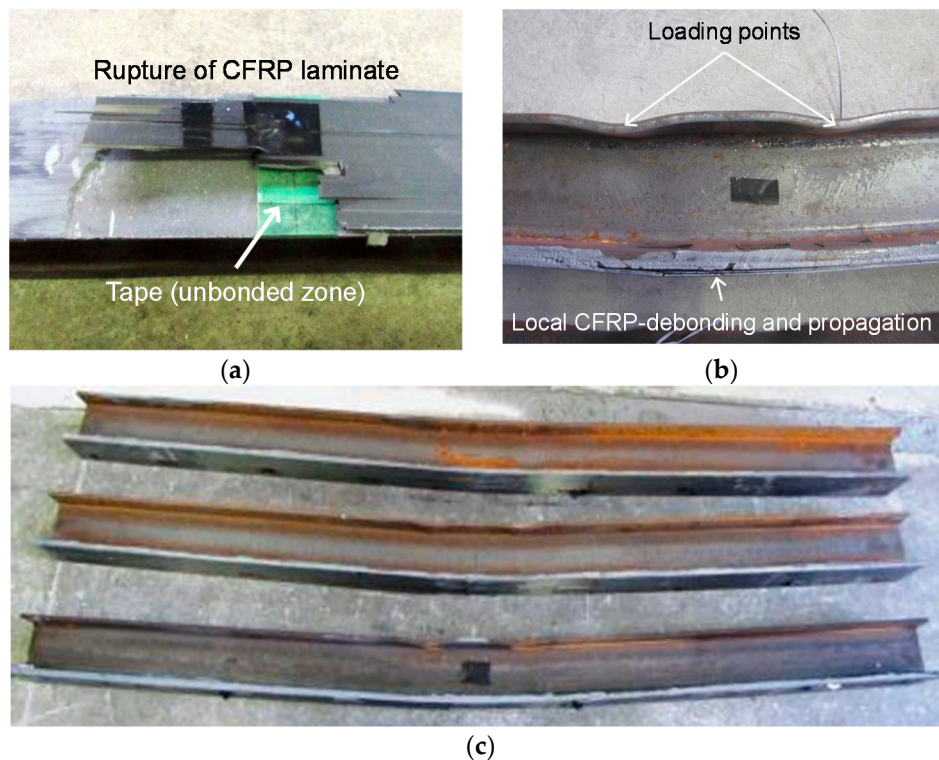


Figure 10. Failure of strengthened beams: (a) rupture of CFRP laminate; (b) Beam B0; (c) Beams B10, B30 and B50.

5. Predictive Assessment

5.1. Interfacial Stress Development

A simple analytical approach may be taken to predict a shear-stress profile along the CFRP-steel interface when subjected to the foregoing temperature loading [11,12].

$$\tau(x) = \frac{1 - \varphi}{2} \cdot c \cdot t_s \cdot E_s \cdot \Delta\varepsilon_t \cdot \frac{\sinh(cx)}{\cosh(cl)} \quad (1)$$

$$\varphi = \frac{1}{1 + E_f t_f / E_s t_s} \quad (2)$$

$$c = \sqrt{\frac{G_a}{t_a}} \cdot \sqrt{\frac{2}{1 - \varphi}} \cdot \frac{1}{\sqrt{E_s t_s}} \quad (3)$$

$$\Delta\varepsilon_t = (\alpha_s - \alpha_f) \cdot \Delta T \quad (4)$$

where $\tau(x)$ is the shear stress of the interface at arbitrary location x ; l is the half-length of the bonded CFRP; t_s , t_a and t_f are the thickness of the steel flange, epoxy adhesive, and CFRP laminate, respectively; E_s and E_f are the elastic moduli of the steel and the CFRP, respectively; G is the shear modulus of the epoxy adhesive; α_s and α_f are the coefficients of thermal expansion of the steel and CFRP, respectively; and ΔT is the temperature variation for the thermal strain. The shear modulus of the epoxy may be determined by fundamental elastic theory using the elastic modulus and Poisson's ratio of the epoxy. Given that the aforementioned equations were derived based on elastic theory, their application range is valid before steel yielding or physical CFRP debonding (outside a full composition action limit). It is important to note again that the purpose of the predictive approach is to examine the interfacial stresses caused by thermal stress during the temperature cycling, rather than by mechanical loading in the residual capacity test.

5.2. Predicted Stress Profile

Figure 11a depicts interfacial stress profiles along the CFRP. Periodic stress peaks were predicted due to the unique bonding scheme explained earlier (Figure 1b). It was assumed that the thermally-induced bending of the steel beam was negligible, even though the CFRP was bonded to only one side of the beam. The reason is that the epoxy is flexible enough (in terms of elastic modulus compared with the steel and the CFRP; Tables 1 and 2) and the CFRP laminate is thin (*i.e.*, the flexural rigidity of the steel beam is significantly greater than that of the CFRP, and hence, virtually no side-confining effect exists). All of the maximum stress values were lower than the shear stress limit of 16 MPa reported by the adhesive manufacturer (CFRP debonding happens when the maximum interfacial shear stress exceeds the shear capacity of the adhesive). The predicted stress profiles theoretically confirmed that the premature CFRP debonding and propagation during the thermal loading period did not take place as discussed in Section 4.1. The contribution of the unbonded zone was not substantial with respect to the stress development, even though the location of maximum stresses shifted from midspan of the beams (Figure 11b). The extent of local CFRP debonding along the interface, therefore, was not an attribute influencing the development of interfacial stress.

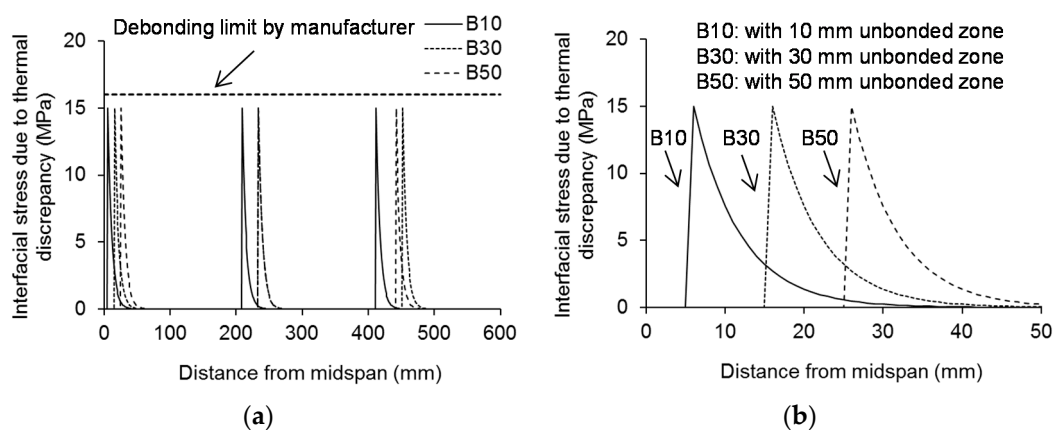


Figure 11. Predicted interfacial shear stress due to thermal loading of $\Delta T = 25\text{ }^{\circ}\text{C}$: (a) from midspan to support; (b) near midspan.

A parametric study was conducted to examine the effect of a temperature difference, as shown in Figure 12a. Typical temperature variation ranges from 10 to 60 $^{\circ}\text{C}$ were considered. Because the stress profiles were repeated periodically, a bond region near a geometric discontinuity was only present. The profile of the interfacial stress was maintained up to a thermal loading of $\Delta T = 20\text{ }^{\circ}\text{C}$, while the initiation of CFRP debonding was noticed at $\Delta T = 30\text{ }^{\circ}\text{C}$ (*i.e.*, the maximum interfacial shear stress reached the debonding limit of 16 MPa). Further increasing the temperature difference resulted in the progression of CFRP debonding. Figure 12b shows the relationship between the

temperature difference and debonding length. A rapid increase in debonding length was noticed when the temperature difference varied from $\Delta T = 30\text{--}40\text{ }^\circ\text{C}$, beyond which a reduced response slope was followed. Such a predicted result illustrates that multiple debonding progression stages can exist when a CFRP-strengthened steel beam is subjected to cyclic temperature loading (sufficiently high ΔT to cause CFRP debonding).

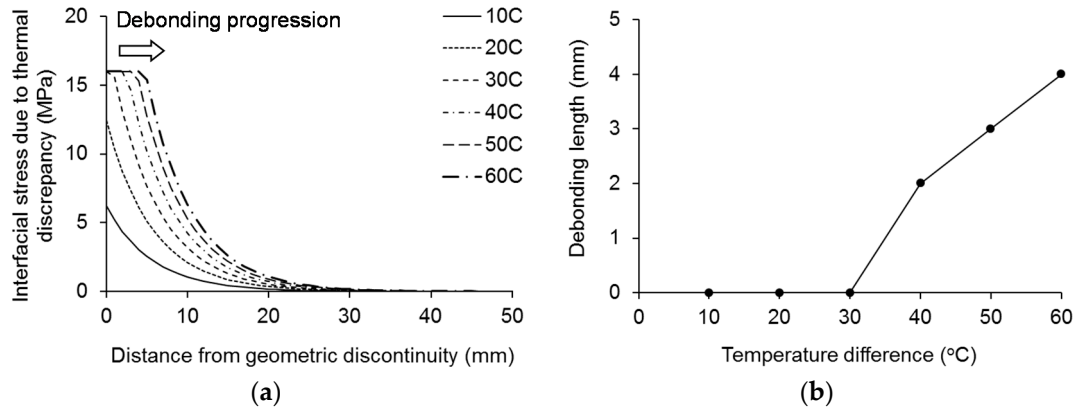


Figure 12. Interfacial stress development depending on temperature difference: (a) stress profile; (b) initiation and propagation of CFRP debonding.

Figure 13 demonstrates the effect of CFRP modulus on interfacial stress development associated with a temperature difference, including two typical ΔT values representing with and without CFRP debonding. The range of CFRP moduli was assumed to vary from 100 to 500 GPa. It is obvious to note that a high modulus CFRP caused a noticeably high interfacial stress, and consequently, synergetic interfacial deterioration (*i.e.*, CFRP debonding due to mechanical stress concentrations and thermal discrepancy) was accompanied as the temperature difference increased. From a practice stand point, the use of a high modulus CFRP may not be recommended for regions experiencing a wide temperature variation range.

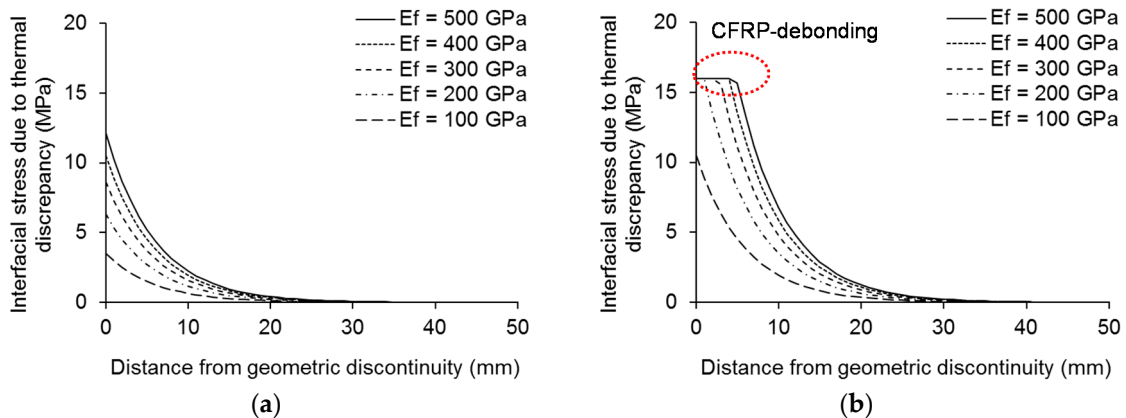


Figure 13. Effect of CFRP modulus: (a) at $\Delta T = 20\text{ }^\circ\text{C}$; (b) at $\Delta T = 60\text{ }^\circ\text{C}$.

6. Summary and Conclusions

This paper has discussed the effect of thermal distress on the residual behavior of CFRP-strengthened steel beams, including periodic unbonded zones, to examine the contribution of local CFRP debonding. A total of 13 beams were tested in flexure after exposing to a cyclic temperature range of $\Delta T = 25\text{ }^\circ\text{C}$ up to 84 days. A simple analytical approach was adopted to

predict interfacial shear stresses between the CFRP and the steel substrate, followed by a numerical parametric study. The following conclusions are drawn:

- The composite action between the CFRP and the substrate was maintained until the strengthened beams were loaded to yielding, irrespective of the extent of thermal cycling and the size of unbonded zones along the interface. With an increase in load level, local damage took place at the geometric discontinuities adjacent to the unbonded zones, and CFRP debonding initiated and progressed.
- The failure of the strengthened beams was attributed to a combination of local flange yielding and CFRP rupture, while the thermal distress effect of $\Delta T = 25\text{ }^\circ\text{C}$ was found to be insignificant. The degree of initial bond defect represented by the unbonded zones appeared to be influential on stress transfer from the steel to the CFRP as the load stage shifted from yielding to ultimate.
- Periodic interfacial stresses were predicted along the CFRP-steel interface due to the presence of the unbonded zones. Such a prediction theoretically confirmed the thermal behavior of the experimental beams (*i.e.*, no progression of CFRP debonding at $\Delta T = 25\text{ }^\circ\text{C}$). The parametric study revealed that CFRP debonding occurred at $\Delta T = 30\text{ }^\circ\text{C}$ and progressed as the temperature difference augmented.
- The possible existence of multiple debonding-progression stages associated with the degree of thermal distress was proposed, while further experimental validation was recommended. High-modulus CFRP laminates should restrictively be used for strengthening steel members if a wide temperature variation range ($\Delta T \geq 30\text{ }^\circ\text{C}$) is anticipated.

Acknowledgments: The authors thank former students (Junpei Itose and Masaya Harada) for their experimental contribution. This paper was invited by the Organizing Committee of the 7th International Conference on FRP Composites in Civil Engineering (CICE-7), and its content was expanded from the conference paper published in the proceedings.

Author Contributions: Isamu Yoshitake and Hisatsugu Tsuda conceived, designed and performed the experiments; Hisatsugu Tsuda and Yail J. Kim analyzed the data; Nobuhiro Hisabe supplied materials; Yail J. Kim and Isamu Yoshitake wrote the paper.

Conflicts of Interest: The authors declare no conflict of interest.

Appendix

The equilibrium of the internal forces may be expressed as:

$$\sigma_s \cdot t_s \cdot b + \sigma_f \cdot t_f \cdot b = 0 \tag{1a}$$

where b is the width of the element; and σ_s and σ_f are the stress of the steel flange and CFRP laminate, respectively.

$$\frac{d\tau_a}{dx} = \frac{G_a}{t_a} \left(\frac{\sigma_s}{E_s} - \frac{\sigma_f}{E_f} + \Delta\varepsilon_t \right) \tag{2a}$$

where τ_a is the shear stress along the adhesive layer induced by the substrate stress. Considering a thin layer of the adhesive, τ_a may be expressed as:

$$\tau_a = \frac{t_s}{2} \cdot \frac{d\sigma_s}{dx} \tag{3a}$$

Substituting Equation (3a) into Equation (2a), the following equation is obtained:

$$\frac{t_s}{2} \cdot \frac{d^2\sigma_s}{dx^2} = \frac{G_a}{t_a} \left(\frac{\sigma_s}{E_s} - \frac{\sigma_f}{E_f} + \Delta\varepsilon_t \right) \tag{4a}$$

Combining Equations (1a) and (4a), one can write:

$$\frac{d^2\sigma_s}{dx^2} - c^2\sigma_s = c^2 \cdot (1 - \varphi) \cdot E_s \cdot \Delta\varepsilon_t \quad (5a)$$

Considering boundary conditions (*i.e.*, symmetric stress of σ_s at $x = 0$ and $\sigma_s = 0$ at $x = l$), the following equation may be obtained:

$$\sigma_s = (1 - \varphi) \cdot E_s \cdot \Delta\varepsilon_t \cdot \left(\frac{\cosh(cx)}{\cosh(cl)} - 1 \right) \quad (6a)$$

Integrating Equations (3a) and (6a) results in Equation (1). It should be noted that Equation (1) may be used for predicting stress development in both FRP termination and local debonding along the bond-line where a stress singularity exists, because their stress state associated with a geometric discontinuity is the same. In the present test program, the singularity occurs immediately beyond the periodic unbonded zone.

References

1. Teng, J.G.; Yu, T.; Fernando, D. Strengthening of steel structures with fiber-reinforced polymer composites. *J. Constr. Steel Res.* **2012**, *78*, 131–143. [[CrossRef](#)]
2. Adams, R.D. *Adhesive Bonding: Science Technology and Applications*; Woodhead Publishing: Cambridge, UK, 2005.
3. Al-Shawaf, A.; Zhao, X.-L. Adhesive rheology impact on wet lay-up CFRP/steel joints' behaviour under infrastructure subzero exposures. *Compos. B Eng.* **2013**, *47*, 207–219. [[CrossRef](#)]
4. Dawood, M.; Rizkalla, S. Environmental durability of a CFRP system for strengthening steel structures. *Constr. Build. Mater.* **2010**, *24*, 1682–1689. [[CrossRef](#)]
5. Al-Shawaf, A. Modelling wet lay-up CFRP-steel bond failures at extreme temperatures using stress-based approach. *Int. J. Adhes. Adhes.* **2011**, *31*, 416–428. [[CrossRef](#)]
6. Nguyen, T.-C.; Bai, Y.; Al-Mahaidi, R.; Zhao, X.-L. Time-dependent behaviour of steel/CFRP double strap joints subjected to combined thermal and mechanical loading. *Compos. Struct.* **2012**, *94*, 1826–1833. [[CrossRef](#)]
7. Rabinovitch, O. Impact of thermal loads on interfacial debonding in FRP strengthened beams. *Int. J. Solids Struct.* **2010**, *47*, 3234–3244. [[CrossRef](#)]
8. Gao, W.Y.; Teng, J.G.; Dai, J.G. Effect of temperature variation on the full-range behavior of FRP-to-concrete bonded joints. *ASCE J. Compos. Constr.* **2012**, *16*, 671–683. [[CrossRef](#)]
9. Gao, W.Y.; Dai, J.G.; Teng, J.G. Analysis of Mode II debonding behavior of fiber-reinforced polymer-to-substrate bonded joints subjected to combined thermal and mechanical loading. *Eng. Fract. Mech.* **2015**, *136*, 241–264. [[CrossRef](#)]
10. Yoshitake, I.; Tsuda, H.; Itose, J.; Hisabe, N. Effect of discrepancy in thermal expansion coefficients of CFRP and steel under cold temperature. *Constr. Build. Mater.* **2014**, *59*, 17–24. [[CrossRef](#)]
11. Okura, I.; Fukui, T.; Nakamura, K.; Matsugami, T. Decrease in stress in steel plates by carbon fiber sheets and debonding shearing stress. *Doboku Gakkai Ronbunshu* **2001**, *689*, 239–249, (In Japanese). [[CrossRef](#)]
12. Tsuda, H. Experimental Study on Bond Properties of Carbon Fiber Reinforced Polymer (CFRP) Laminate Glued to Steel Substrate under Cold Temperature. Ph.D. Thesis, Yamaguchi University, Ube, Japan, March 2015. (In Japanese).



© 2015 by the authors; licensee MDPI, Basel, Switzerland. This article is an open access article distributed under the terms and conditions of the Creative Commons by Attribution (CC-BY) license (<http://creativecommons.org/licenses/by/4.0/>).